JOURNAL OF Evolutionary Biology

doi: 10.1111/jeb.12932

Otolith shape lends support to the sensory drive hypothesis in rockfishes

V. M. TUSET*, J. L. OTERO-FERRER†, J. GÓMEZ-ZURITA‡, L. A. VENERUS§, C. STRANSKY¶, R. IMONDI**, A. M. ORLOV††‡‡§§, Z. YE¶¶, L. SANTSCHI**, P. K. AFANASIEV††, L. ZHUANG¶¶, M. FARRÉ*, M.S. LOVE*** & A. LOMBARTE*

*Instituto de Ciencias del Mar (CSIC), Barcelona, Spain
†Departamento de Ecoloxía e Bioloxía Animal, Universidad de Vigo, 36310 Vigo (Pontevedra), Spain
‡Institute of Evolutionary Biology, CSIC-Universitat Pompeu Fabra, Barcelona, Spain
§Centro para el Estudio de Sistemas Marinos (CESIMAR), Centro Nacional Patagónico (CENPAT-CONICET), Puerto Madryn, Chubut, Argentina
¶Thünen Institute of Sea Fisheries, Hamburg, Germany
**Coastal Marine Biolabs, Integrative Biosciences Program, Ventura, CA, USA
††Russian Federal Research Institute of Fisheries and Oceanography, Moscow, Russia
‡‡A.N. Severtsov Institute of Ecology and Evolution, Moscow, Russia
§§Department of Ichthyology, Faculty of Biology, Dagestan State University, Makhachkala, Russia
¶¶Fisheries College, Ocean University of China, Qingdao, China
***Marine Science Institute, University of California, Santa Barbara, CA, USA

Keywords:

adaptation;
ecology;
otolith shape;
phylogeny;
rockfishes;
sensory drive hypothesis.

Abstract

The sensory drive hypothesis proposes that environmental factors affect both signalling dynamics and the evolution of signals and receivers. Sound detection and equilibrium in marine fishes are senses dependent on the *sagittae* otoliths, whose morphological variability appears intrinsically linked to the environment. The aim of this study was to understand if and which environmental factors could be conditioning the evolution of this sensory structure, therefore lending support to the sensory drive hypothesis. Thus, we analysed the otolith shape of 42 rockfish species (*Sebastes* spp.) to test the potential associations with the phylogeny, biological (age), ecological (feeding habit and depth distribution) and biogeographical factors. The results showed strong differences in the otolith shapes of some species, noticeably influenced by ecological and biogeographical factors. Moreover, otolith shape was clearly conditioned by phylogeny, but with a strong environmental effect, cautioning about the use of this structure for the systematics of rockfishes or other marine fishes. However, our most relevant finding is that the data supported the sensory drive hypothesis as a force promoting the radiation of the genus *Sebastes*. This hypothesis holds that adaptive divergence in communication has significant influence relative to other life history traits. It has already been established in *Sebastes* for visual characters and organs; our results showed that it applies to otolith transformations as well (despite the clear influence of feeding and depth), expanding the scope of the hypothesis to other sensory structures.

Introduction

An adaptive radiation is the diversification of an ancestral species into several descendant species, each one morphologically and physiologically adapted to a different ecological niche. This typically occurs in a short evolutionary time interval (Losos, 2010). Parallel adaptive radiations of related organisms frequently produce convergent forms, resulting from adaptation to similar ecological conditions (Rüber & Adams, 2001), although the same process may also occur across phylogenetically distant groups (Winemiller, 1991). Exploring the association between environmental factors and the

Correspondence: Victor Manuel Tuset, Instituto de Ciencias del Mar (CSIC), Passeig Marítim de la Barceloneta 37-49, 08003 Barcelona, Catalonia, Spain.
Tel.: +34 932 300 500; fax: +34 932 309 555;
e-mail: vtuset@icm.csic.es

morphology of organisms is a central theme in evolutionary biology and may help understanding the radiation of clades, their evolution and diversity (Klingenberg & Ekau, 1996; Ricklefs & Bermingham, 2007; Langerhans, 2010). There is a growing interest in expanding these studies to the analysis of sensory structures and their role in adaptive radiations. Divergent signals play a key role in the establishment and maintenance of premating reproductive isolation, and the processes driving signal divergence are therefore clearly relevant to studies of speciation and species co-existence (Endler, 1992; Boughman, 2002). Marine fishes can develop different sensory perceptions, segregate their activity rhythms and have lifespan trade-offs facilitating coexistence (Mangel *et al.*, 2007; Pulcini *et al.*, 2008). Therefore, it might be expected that these effects would mirror in the various sensory systems (Lombarte *et al.*, 2003; Seehausen *et al.*, 2008). The idea that speciation may be heavily promoted by the diversification of sensory interactions of organisms with their environment was formalized as the so-called sensory drive hypothesis (Endler, 1992, 1993). Thus, under sensory drive, a female is more likely to choose a male whose mating signature can be more easily detected by her sensory apparatus (Endler & Houde, 1995; Kawata *et al.*, 2007; Seehausen *et al.*, 2008).

In this framework, otoliths or 'ear bones' of fishes are biological structures amenable to ecomorphological analyses that become an appealing target for studies of the association between sensory processes and diversification. They are located in the inner ear of vertebrates and act as sound detectors as well as organs of equilibrium (Popper & Fay, 2011). Otoliths consist of three pairs of calcareous structures – the *sagittae*, *lapilli* and *asterisci* each contained within individual vestibules of the labyrinth compartments (Fay & Popper, 2012). *Sagittae* otoliths show strong morphological variability associated with phylogenetic factors (Nolf, 1985); life history traits (Volpedo & Echeverria, 2003); ecological, biological and behavioural traits (Torres *et al.*, 2000; Lychakov & Rebane, 2000; Lombarte *et al.*, 2010); type of substrate (Volpedo & Echeverria, 2003); and other environmental factors (Castonguay *et al.*, 1991; Schulz-Mirbach *et al.*, 2008; Vignon & Morat, 2010). These biological structures have sufficiently conservative characters (i.e. type of sulcus, ratio between sulcus and otolith area, type of otolith; see Tuset *et al.*, 2008) to be markedly species-specific (Gaemers, 1984; Nolf, 1985; Lombarte *et al.*, 1991; Stransky & MacLellan, 2005). Thus, this specific character may be suitable for analysing the impact of phylogeny on the *sagittae* shape (Lombarte *et al.*, 1991; Lombarte & Castellón, 1991; Schwarzhans, 2014). However, there are no studies that have formally evaluated the influence of phylogeny on otolith shape variation, as has been performed for other anatomical structures of fishes such as the cranium, the feeding apparatus or general body shape (Rüber & Adams, 2001; Price *et al.*, 2011). Lombarte *et al.* (2010), using antarctic and subantarctic nototheniids, pioneered considerations of phylogenetic inertia — that is, the tendency for related species to have similar morphological features acquired from the common ancestral species — in the study of otolith shape. However, they found only a weak association between otolith shape and phylogeny, but a strong correspondence with the trophic niche of the species. Certainly, otoliths have received considerable attention and are used for different purposes; hence, it is important to identify and quantify the relative importance of the factors affecting their morphological variability (Vignon, 2015).

The rockfishes (*Sebastes* spp.) form a clade of about 110 species which live in diverse marine habitats worldwide (Kendall, 2000; Nelson, 2006). This genus contains a number of sibling species pairs and incipient species indicating ongoing speciation processes (Hyde *et al.*, 2008; Stefánsson *et al.*, 2009; Venerus *et al.*, 2013). Habitat, depth distribution, feeding habit and swimming activity are features that, taken together, likely have had an influence on their diversification (Ebeling *et al.*, 1980; Love & York, 2005; Love *et al.*, 2009). For these reasons, this group has attracted the attention of ecologists, evolutionary biologists and phylogeneticists (Rocha-Olivares *et al.*, 1999; Mangel *et al.*, 2007; Ingram & Shurin, 2009; Magnuson-Ford *et al.*, 2009; Ingram, 2011; Venerus *et al.*, 2013). Most species of *Sebastes* occur in the eastern and western North Pacific. Regarding the few species that reside in the North Atlantic, the currently accepted hypothesis is that they derive from a colonization from the North Pacific. According to this hypothesis, an ancestral species moved eastwards during the 'great transarctic biotic interchange', when the Bering land bridge opened and Arctic waters warmed up, allowing the movement of sub-boreal species through the Arctic Ocean (Rocha-Olivares *et al.*, 1999; Love *et al.*, 2002; Hyde & Vetter, 2007). Expansion into the Southern Hemisphere occurred through the Eastern Tropical Pacific followed by spreading around the Pacific and Atlantic coasts of South America, probably through a unique colonization event or at least during a short time interval by members of the same evolutionary lineage (Eschmeyer & Hureau, 1971; Rocha-Olivares *et al.*, 1999). Interestingly, this zoogeographic hypothesis also received support from the analysis of variation of *sagittae* shape in eleven rockfish species (Stransky & MacLellan, 2005). The role of environmental differences leading to diversification in this group has also been demonstrated for morphological differences associated with differential distribution in depth gradients (Ingram, 2011). And highly relevant for the purposes of this study, the sensory drive hypothesis had been suggested already as a promoter of speciation in rockfishes by recognizing changes in the sequence of amino acids of eye

rhodopsins (Sivasundar & Palumbi, 2010) and in otolith shapes (Tuset *et al.*, 2015; Zhuang *et al.*, 2015) along a depth gradient.

Here, we perform the first study aimed at validating the sensory drive hypothesis in *Sebastes* using morphological variation in a hearing structure, the otolith, by evaluating the role of phylogeny, ecology and biogeography on the interspecific variability of otolith shape. We propose that an association between morphological variability of otoliths and environmental factors beyond the restrictions imposed by phylogeny can lend support to the hypothesis.

Materials and methods

Data collection

Many studies have analysed several aspects of the evolution of *Sebastes*. Here we aimed at the largest taxonomic coverage investigated so far, analysing 42 species of *Sebastes* representing 14 lineages from widespread geographical areas of the Pacific and Atlantic Oceans, both in the Northern and Southern Hemispheres. Otolith images for every species were available thanks to the activity of several research groups (see Stransky & MacLellan, 2005; Orlov & Tokranov, 2006; Zhuang *et al.*, 2015; Tuset *et al.*, 2015). Data on species, their origin, number of specimens per species, their assignment to subgenera or clades according to Hyde & Vetter (2007), ecological characteristics of habitat and otolith length summary data are listed in Table 1.

Geographical ranges given for each species follow the classification by Magnuson-Ford *et al.* (2009): northwest Pacific, north Pacific, northeast Pacific, southern northeast Pacific, eastern central Pacific, northwest Atlantic, north Atlantic, northeast Atlantic, southwest Pacific and southeast Atlantic. Depth and predation strategy seem to affect otolith shape (Tuset *et al.*, 2015), and we compiled relevant data on feeding habits, depth range and maximum age, although longevity data were missing for some species (see Table 1). Feeding habits were compiled from data in Hallacher & Roberts (1985), Love *et al.* (1990), Horinouchi & Sano (2000) and Jin (2006), and were divided into three categories based on each prey's trophic level (Linde *et al.*, 2004): planktonic prey (i.e. amphipods, isopods, copepods and euphausiids), nektonic prey (i.e. cephalopods, fishes) or mobile-benthic prey (i.e. polychaetes, gastropods, bivalves, brachyurids, ophiuroids, decapods and echinoids). We assumed that feeding habit is representative of each species during their adult life stage, as usual in this kind of ecological studies (Anderson *et al.*, 2009). Depth data were defined as the maximum depth of the maximum abundance range (Love *et al.*, 2002; Ingram & Shurin, 2009; Froese & Pauly, 2015). For species lacking this information, we predicted maximum common depth from a log-regression equation of maximum common depth against absolute maximum depth ($r^2 = 0.723$, $n = 35$, $P < 0.001$; Ingram & Shurin, 2009). Maximum age data were not available for four species (Table 1; Froese & Pauly, 2015), but this variable was included in the analyses because longevity is an ecological parameter indicating the persistence of a population in a variable environment (Berkeley *et al.*, 2004).

Phylogenetic analysis

Phylogenetic trees were obtained from a sample of 44 individuals representing 42 species of *Sebastes* as well as two outgroups, *Helicolenus avius* Abe & Eschmeyer, 1972 and *Hozukius emblemarius* (Jordan & Starks, 1904). For each individual, we obtained the public available sequences of eight loci from Hyde & Vetter (2007) including several nonprotein coding mitochondrial (D-loop, *rrnL*, *rrnS*, tRNA-Thr/tRNA-Pro) and nuclear (*its*1) genes and protein coding mitochondrial (*cob*, *cox1*) and nuclear (*rag2*) genes (Table S1). Each locus was aligned independently from the others using the G-INS-i algorithm in MAFFT 7 (Katoh *et al.*, 2002), and all loci were concatenated in a single matrix encompassing 5439 nucleotide positions, 3% of which included gaps (only in the D-loop and its1 partitions). Two tree inference procedures, maximum likelihood and Bayesian inference, were assayed on these data to estimate phylogenetic distances between pairs of species, measured as their intervening branch lengths (i.e. patristic distances). Prior to the phylogenetic analyses, we estimated the optimal model of evolution for each locus independently using jModelTest 2.1.3 (Darriba *et al.*, 2012). Maximum likelihood trees were obtained using partitioned models for each locus to generate both the optimal tree and a measure of node support based on 500-bootstrap pseudoreplicates using RAxML 7.2.8 (Stamatakis, 2006). Bayesian tree inference was carried out using MrBayes 3.2.2 (Ronquist *et al.*, 2012) whereby tree searches used two replicates with four Markov Chain Monte Carlo chains of 50M generations each, subsampling trees every 5000 generations, with independent evolutionary models for each partition. Trees and parameters of interest were obtained from the posterior output of MrBayes after conservatively discarding 10% of the initial trees.

Otolith shape analysis

The shape of 847 left otoliths was analysed using wavelet functions. A total of 512 equidistant Cartesian coordinates for each otolith were extracted – each contour was originated in the *rostrum* (see otolith terminology in Tuset *et al.*, 2008) – and analysed using the wavelet transformed (WT; see Parisi-Baradad *et al.*, 2005). Image processing was performed using the image analysis software Age and Shape (version 1.0; Infaimon SL®, Barcelona, Spain). For each contour, nine wavelets

Table 1 Ecological and morphometric data on rockfishes collected from both hemispheres.

								Otolith length (mm)	
Subgenus	Species	Acronym	Area	Feeding	Depth	Age	*n*	Range	Mean (SE)
–	*S. elongatus*	elo	NEP	Plank-Nek	366	54	4	8.00–11.43	8.88 (0.85)
Acutomentum	*S. hopkinsi*	hop	SNEP	Plank	150	19	13	6.51–12.93	8.78 (0.46)
Acutomentum	*S. ovalis*	ova	SNEP	Plank-Nek	150	37	9	9.09–13.20	10.79 (0.49)
Clade A	*S. proriger*	pro	NP	Plank-Nek	274	55	30	12.44–15.30	14.01 (0.12)
Clade B	*S. borealis*	bor	NP	Mob-Nek	750	157	30	12.11–19.60	15.72 (0.28)
Clade B	*S. brevispinis*	bre	NEP	Plank-Nek	300	82	30	15.20–19.60	17.51 (0.24)
Clade B	*S. iracundus*	ira	NWP	Mob-Nek	800	–	20	16.48–23.13	19.17 (0.32)
Clade D	*S. semicinctus*	sem	SNEP	Plank	149	15	15	6.34–9.20	7.68 (0.17)
Mebarus	*S. thompsoni*	tho	NWP	Plank-Nek	150	–	30	7.53–11.03	8.94 (0.14)
Pteropodus	*S. atrovirens*	atr	SNEP	Mob	12	25	14	9.46–10.55	9.86 (0.25)
Pteropodus	*S. auriculatus*	aur	NEP	Mob	53	34	18	6.93–11.20	9.49 (0.29)
Pteropodus	*S. carnatus*	car	SNEP	Mob	37	30	16	7.62–9.35	8.47 (0.12)
Pteropodus	*S. caurinus*	cau	NEP	Mob	119	55	16	7.66–12.00	9.61 (0.49)
Pteropodus	*S. chrysomelas*	chr	NEP	Mob	18	30	4	7.41–8.65	8.15 (0.27)
Rosicola	*S. miniatus*	min	NEP	Mob-Nek	274	60	5	8.67–15.97	12.35 (1.29)
Sebastes	*S. alutus*	alu	NP	Plank-Nek	293	103	30	13.80–18.30	15.53 (0.19)
Sebastes	*S. ciliatus*	cil	NP	Mob-Plank	106	67	5	12.44 -17.27	14.74 (0.82)
Sebastes	*S. fasciatus*	fas	NWA	Mob-Plank	366	32	30	10.80 –17.50	14.01 (0.37)
Sebastes	*S. mentella*	men	NA	Plank-Nek	789	71	30	14.20 –18.90	15.92 (0.22)
Sebastes	*S. norvegicus*	nor	NEA	Plank-Nek	500	45	30	12.80 –16.90	14.20 (0.21)
Sebastes	*S. polyspinis*	pol	NP	Plank-Nek	400	57	15	10.35–16.70	14.06 (0.43)
Sebastes	*S. reedi*	ree	NEP	Mob-Nek	366	99	30	13.27–-16.21	14.89 (0.14)
Sebastes	*S. viviparus*	viv	NEA	Mob-Nek	188	40	20	8.50–11.10	9.58 (0.18)
Sebastichthys	*S. rubrivinctus*	rub	SNEP	Mob-Nek	183	45	24	7.27–12.83	10.14 (0.41)
Sebastichthys	*S. serriceps*	ser	SNEP	Mob-Nek	60	25	10	7.53–10.84	9.17 (0.32)
Sebastocles	*S. hubbsi*	hub	NWP	Mob	150	8	30	4.78–6.45	5.61 (0.07)
Sebastocles	*S. schlegeli*	sch	NWP	Mob-Nek	250	26	30	6.44–8.11	7.36 (0.07)
Sebastodes	*S. goodei*	goo	NEP	Plank-Nek	250	35	6	7.25–10.11	8.34 (0.41)
Sebastodes	*S. paucispinis*	pau	NEP	Nek	250	50	15	10.02–11.90	10.85 (0.44)
Sebastomus	*S. capensis*	cap	SEA	Mob	174	18	30	11.95–15.46	13.41 (0.16)
Sebastomus	*S. chlorostictus*	chl	NEP	Plank-Nek	201	33	18	7.69–14.72	10.08 (0.41)
Sebastomus	*S. constellatus*	con	SNEP	Mob-Nek	149	32	7	9.05–11.72	10.19 (0.43)
Sebastomus	*S. ensifer*	ens	SNEP	Plank	239	–	11	7.60–9.23	8.49 (0.18)
Sebastomus	*S. oculatus*	ocu	SWA	Mob-Nek	60	–	30	7.87–13.69	11.87 (0.26)
Sebastomus	*S. rosaceus*	ros	NEP	Mob	46	18	15	8.23–12.58	9.88 (0.28)
Sebastomus	*S. umbrosus*	umb	ECP	Plank-Nek	70	–	9	8.20–11.19	10.02 (0.28)
Sebastosomus	*S. entomelas*	ent	NEP	Plank-Nek	327	60	30	13.42–18.93	16.96 (0.24)
Sebastosomus	*S. flavidus*	fla	NEP	Plank-Nek	46	64	30	16.25–21.39	18.64 (0.22)
Sebastosomus	*S. mystinus*	mys	NEP	Plank-Nek	550	44	20	7.84–12.86	10.05 (0.58)
Zalopyr	*S. glaucus*	gla	NP	Plank-Nek	250	32	29	8.63–16.53	12.30 (0.39)
Zalopyr	*S. melanostictus*	mel	NEP	Nek	450	205	30	15.16–24.40	18.64 (0.39)
Zalopyr	*S. owstoni*	ows	NWP	Plank-Nek	350	20	29	7.89–10.67	9.50 (0.15)

The subgenera followed Kendall (2000) and Hyde & Vetter (2007). *n*, number of specimens; SE, standard error. The geographical range followed Magnuson-Ford *et al.* (2009): north-west Pacific (NWP), north Pacific (NP), north-east Pacific (NEP), southern northeast Pacific (SNEP), eastern central Pacific (ECP), north-west Atlantic (NWA), north Atlantic (NA), north-east Atlantic (NEA), south-west Atlantic (SWA) and south-east Atlantic (SEA). Feeding habit categories were proposed by Linde *et al.* (2004): planktonic (Plank), nektonic (Nek) or mobile benthic prey (Mob). Age and depth were taken from Froese & Pauly (2015).

were obtained depending on the degree of otolith detail; however, for the purpose of this study, the 5th wavelet scale was selected because it expressed the specific characters better than the other wavelet scales (Tuset *et al.*, 2015).

A principal component analysis (PCA) based on the variance–covariance matrix was performed to reduce the wavelet functions without losing information (Tuset *et al.*, 2015). Significant eigenvectors were identified plotting the percentage of total variation explained by the eigenvectors vs. the proportion of variance expected under the 'broken-stick model' (Gauldie & Crampton, 2002). Interspecific differences that might be attributed to allometry were tested using Pearson's correlations

between otolith length and the principal components (Stransky & MacLellan, 2005). The effect of otolith length was removed using the residuals of the common within-group slopes of the linear regressions of each component on otolith length, building a new PCA matrix.

Morphometric differences in the shape of otoliths in rockfishes were detected by means of multivariate analyses. Canonical variate analysis (CVA) was computed on the reduced PCA matrix to summarize the variation between species maximizing their distances (Linde *et al.*, 2004). Moreover, otoliths were classified using a leaving-one-out cross-validation on the classifier matrix, whereby a concordance between classification success rates in the nonvalidated and validated analyses (obtained from the confusion matrix, *sensu* Kohavi & Provost, 1998) indicates that group discrimination was not based on a one-case contribution (Tabatabaei Yazdi & Adriaens, 2013). Finally, otolith morphotypes were defined arranging the species according to their similarity in morphospace using the centroids of the CVA axes (Linde *et al.*, 2004; Tuset *et al.*, 2015). Clustering of otoliths was performed using three methods: (i) unweighted pair group method of arithmetic averages algorithm (UPGMA) from Euclidean distances, (ii) Ward's method and (iii) neighbour-joining algorithm from Euclidean distances and supported by a confidence assessment based on 10 000-bootstrap pseudoreplicates (Legendre & Legendre, 1998).

Phylogenetic patterns of shape variation

Three methods were used to analyse the possible association of otolith shape with the phylogeny of rockfish species. The first method was based on visualizing which morphological groups were congruent with those defined by phylogeny (Clabaut *et al.*, 2007). The second method evaluated the correlation between pairwise phylogenetic patristic distances and morphological distances using a normalized Mantel test (Mantel, 1967), calculated over 10 000 random matrix permutations (Legendre & Legendre, 1998). As maximum likelihood and Bayesian approaches produced very similar phylogenetic trees (see results), the patristic distances used to evaluate phylogenetic influence were those obtained from the maximum likelihood tree. The third method was based on the analysis of correlation between phylogenetic data and canonical variables as defined above. A principal coordinates analysis (PCoA) was performed on the phylogenetic distance matrix, resulting in new transformed variables (F1, F2, ..., F20) which ordered samples according to phylogenetic distance. Next, this new set of variables was correlated with canonical variables (CVA1, CVA2, ..., CVA20) using redundancy analysis (RDA), which is the direct extension of multiple regression applied to modelling multivariate response data (Legendre & Legendre, 1998). Canonical coefficients for the explanatory variables on each axis were used as the criteria to highlight the most important variables explaining the different axes. The statistical significance of correlations extracted from the RDAs was estimated using a Monte Carlo permutation test with 10 000 simulations (Ibánez *et al.*, 2007). For this analysis, 20 phylogenetic and canonical variables were used, which explained 85.4% and 97.3% of the total variance, respectively. The analyses were carried out using XLSTAT-ADA and XLSTAT-PRO software (Addinsoft version 2015.3.01).

Test of phylogenetic inertia on otolith shape

The association between otolith shape and ecological factors (area, depth, feeding and age), subtracting the effect of similarity due to phylogeny, was examined using a phylogenetic generalized least squares (PGLS) analysis implemented in the R package *caper* (Orme *et al.*, 2012). In the model, delta (δ, change in evolutionary rates) and kappa (κ, gradual vs. punctuated evolution) were fixed at 1 (assuming Brownian motion in both cases), whereas lambda (λ, the strength of phylogenetic signal) was specified considering three hypotheses: $\lambda = 0$, indicating lack of phylogenetic signal in otolith shapes; $\lambda = 1$, suggesting that the pattern of morphological similarity between species is proportional to the time of common ancestry under a Brownian motion model of evolution; and $0 < \lambda < 1$, where the intermediate value of λ denotes different strength of the phylogenetic signal. In the latter scenario, the optimal value of λ was estimated using a maximum likelihood (ML) approach (Pagel, 1999; Freckleton *et al.*, 2002), and we used likelihood ratio tests to find significant differences between the ML-estimated value of λ and the three null models (Freckleton *et al.*, 2002). The phylogenetic signal was obtained from the eigenanalysis of the phylogenetic variance–covariance matrix of species (Linde *et al.*, 2004). The degree of relatedness of the diagonal elements of the matrix (the 'variances') was the sum of branch lengths from the root to the tips of the tree for each species, whereas the off-diagonal values (the 'covariances') were the sum of branch path lengths from the root to the last common ancestor for each pair of species (Pagel, 1999; Freckleton *et al.*, 2002). To test the effects of the above-mentioned factors on otolith shape, each factor was regressed on the CVA matrix. Nevertheless, the number of canonical variables analysed was restricted to the first four variables because they were the best correlated with phylogeny (see results). Moreover, explanatory variables were also regressed on shape using more complex models that included all factors (Clabaut *et al.*, 2007).

Results

Phylogeny of *Sebastes*

The molecular markers selected for phylogenetic inference could be divided into five groups according to their evolutionary dynamics, which was taken into account for phylogenetic inference under both maximum likelihood and Bayesian approaches: a GTR + G + I model showed best fit for *cob*, *cox1* and the D-loop region; a GTR + I for the *rrnL* locus; a GTR + G for *its1*; HKY + G + I for *rrnS* and *rag2*; and HKY + I for the mtDNA tRNA loci. Both phylogenetic inference approaches supported very similar tree topologies (likelihood ML tree: −22 980.43; harmonic mean of likelihood of BI trees [stationary phase]: −23 122.07 and −23 122.01), with similar branch lengths and supports (Fig. 1) and coincident with that obtained by Hyde & Vetter (2007). The only topological differences affected an area without support and resolution, with very short branches, therefore with little effect on the estimation of patristic distances. In the ML tree, *S. miniatus* appeared in a polytomy including the clades corresponding to the subgenera *Sebastomus, Sebastichthys* and *Acutomentum*, whereas in the BI tree, a group of species in *Sebastomus* (*S. entomelas* and relatives) was placed as sister to this assemblage.

Phenotypic diversity of *Sebastes* otoliths

The first 20 components of the PCA analysis accounted for higher variance than expected by chance alone (97.3%). Components were not considerably reduced in number; in fact, the first four components only comprised 53.5% of the variance (Table S2). The canonical variate analysis revealed the existence of significant differences between species (Wilks's $\lambda = 6.244 \times 10^{-4}$, d.f.1 = 820, d.f.2 = 1.40×10^{4}, $P < 0.001$). The projection of the centroid scores onto the first two canonical variates (CVA 1 = 41.4%; CVA 2 = 13.4%) showed a clear separation of Atlantic redfishes (*S. fasciatus*, *S. norvegicus, S. mentella* and *S. viviparus*) and some species from the north Pacific (*S. borealis*) and north-west Pacific (*S. iracundus* and *S. owstoni*) from all other species (Fig. 2). Although otolith shapes were clearly separated spatially, most of the species were close in morphospace. Remarkably, species which are distant geographically but close evolutionarily, such as *S. capensis* (southeast Atlantic) and *S. oculatus* (south-east Pacific and south-west Atlantic), were not isolated within morphospace. On average, the percentage of correct assignment was 58.1%, and it was not correlated with the number of specimens available for each species (linear regression, $r^2 = 0.146$, $P > 0.05$); only in the case of twelve species, it reached 70%, and in six cases, it was below 30% (Table S3). Specifically, 28.6% of the

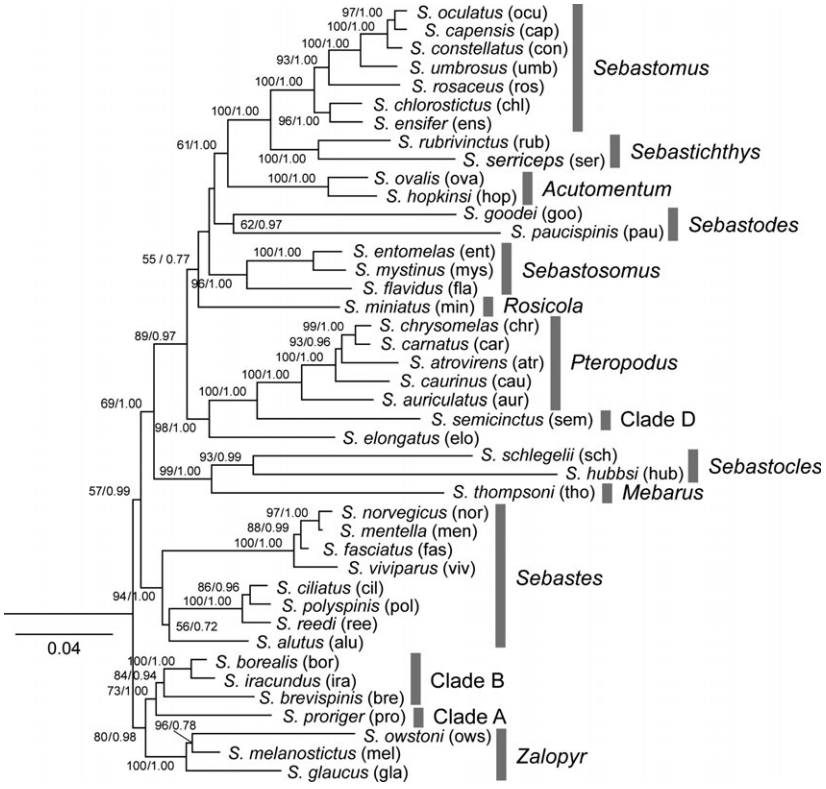

Fig. 1 Optimal tree obtained from the combined maximum likelihood analysis of eight loci including ribosomal and protein coding genes of both the mtDNA and nuclear genomes of *Sebastes*. The tree was rooted with the homologous sequences from species in closely related genera (*Helicolenus avius* and *Hozukius emblemarius*), and these outgroups were removed secondarily. Numbers next to nodes represent bootstrap support values > 50% and clade posterior probabilities > 0.70 as obtained from a Bayesian analysis of the same data. Species codes are given as in Table 1, and the subgenera of *Sebastes* are indicated following the classifications of Kendall (2000) and Hyde & Vetter (2007).

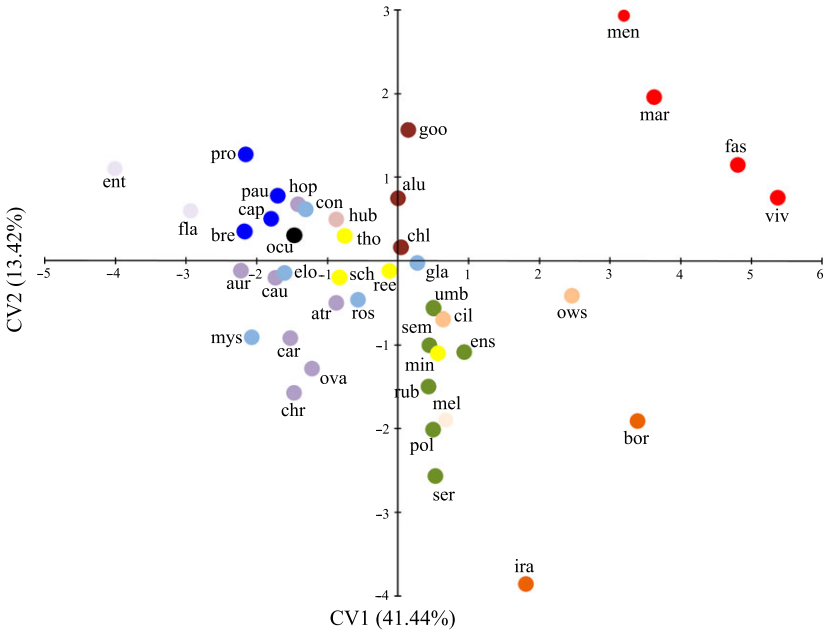

Fig. 2 Morphospace of otolith shapes from canonical variate analysis. Different colours indicate the geographical designation according to Magnuson-Ford *et al.* (2009): north-west Pacific (in yellow), north Pacific (green), north-east Pacific (dark blue), southern north-east Pacific (violet), eastern central Atlantic (light blue), north-west Atlantic (light orange), north Atlantic (red), north-east Atlantic (dark orange), south-west Atlantic (black) and south-east Atlantic (cream). The species are identified with their acronyms as shown in Table 1 and Fig. 1.

otoliths of *S. (Pteropodus) atrovirens* were assigned to *S. (Pteropodus) carnatus*; and 22.2% of the otoliths of *S. (Sebastomus) umbrosus* were misclassified either as *S. (Sebastomus) ensifer* or *S. (Sebastomus) chlorosticus*, likely because the latter three species can be found together in the same reefs.

Although each method provided somewhat different results, cluster analyses essentially separated otoliths into two dominant shapes: elliptic and fusiform. The clusters obtained using the UPGMA method did not strictly explain this morphological variability. For example, several species with elliptic otoliths (i.e. *S. umbrosus* or *S. semicinctus*) were placed in the same group as some species with elongated ones (i.e. *S. rosaceus* or *S. brevispinis*; Fig. 3a). In this case, it is likely that this method considered the width of the otolith as the main factor for clustering. In contrast, both Ward's method and the neighbour-joining algorithm revealed two large groups of otoliths both placing the emphasis on the maximum width perpendicular to the antero-posterior axis (in the middle of the otolith or closer to the anterior zone), and the size of the posterior axis relative to the anterior one. The most noticeable disparity between the latter two methods affected two groups. With Ward's method, one group included the species *S. goodei*, *S. chlorostictus*, *S. alutus*, *S. hubbsi* and *S. oculatus*, whose otoliths were classified as elliptic (Fig. 3b). With the neighbour-joining algorithm, the similarities between *S. goodei*, *S. chlorostictus*, *S. alutus* and *S. hubbsi* were also identified; however, *S. oculatus* was classified together with species having fusiform otoliths (Fig. 3c). Based on these results, we considered that morph identifications obtained with the neighbour-joining algorithm were more accurate, because the otoliths of *S. hubbsi* were wider, and therefore more elliptic, than these of *S. oculatus*. Thus, using the neighbour-joining algorithm, we identified nine morphs that encompassed more than one species, plus two shapes that were quite different and exclusive to a single species each (i.e. *S. hubsii* and *S. oculatus*; Fig. 4). In turn, these nine morphs split into two large morphological groups (I–V and VI–IX), which differed in their degree of ellipticity (Fig. 4). The nine morphs considered in our interpretations of data are as follows: morph I, elliptic–pentagonal shape with conspicuous growth of the otolith in width, large *rostrum*, and wide *antirostrum* and *excisura ostii* (*S. viviparus*, *S. fasciatus*, *S. norvegicus* and *S. mentella*); morph II, similar to morph I, but with narrower *antirostrum* and *excisura* (*S. borealis*, *S. iracundus*, *S. ciliatus*, *S. melanostictus* and *S. owstoni*); morph III, typically elliptic with or without *excisura*, short and rounded *rostrum*, absent or short *antirostrum* and widest at middle (*S. polyspinis*, *S. serriceps*, *S. rubrivinctus*, *S. semicinctus*, *S. umbrosus* and *S. ensifer*); morph IV, elliptic–oblong shape, more prominent *rostrum* and *antirostrum* with an acute notch (*S. reedi*, *S. schlegeli*, *S. thompsoni* and *S. miniatus*); morph V, markedly elliptic shapes with narrower anterior and posterior zones, and large and pointed *rostrum* (*S. goodei*, *S. chlorostictus* and *S. alutus*); morph VI, elliptic–oblong where the dorsal-anterior zone is wider, short *rostrum*, and absent or short *antirostrum*, without notch (*S. ovalis*, *S. chrysomelas*, *S. carnatus*, *S. caurinus*, *S. auriculatus*, *S. atrovirens* and *S. hopkinsi*); morph VII, oblong with large and pointed *rostrum* (*S. flavidus* and *S. entomelas*); morph VIII, fusiform shape with a well-defined, large, broad and

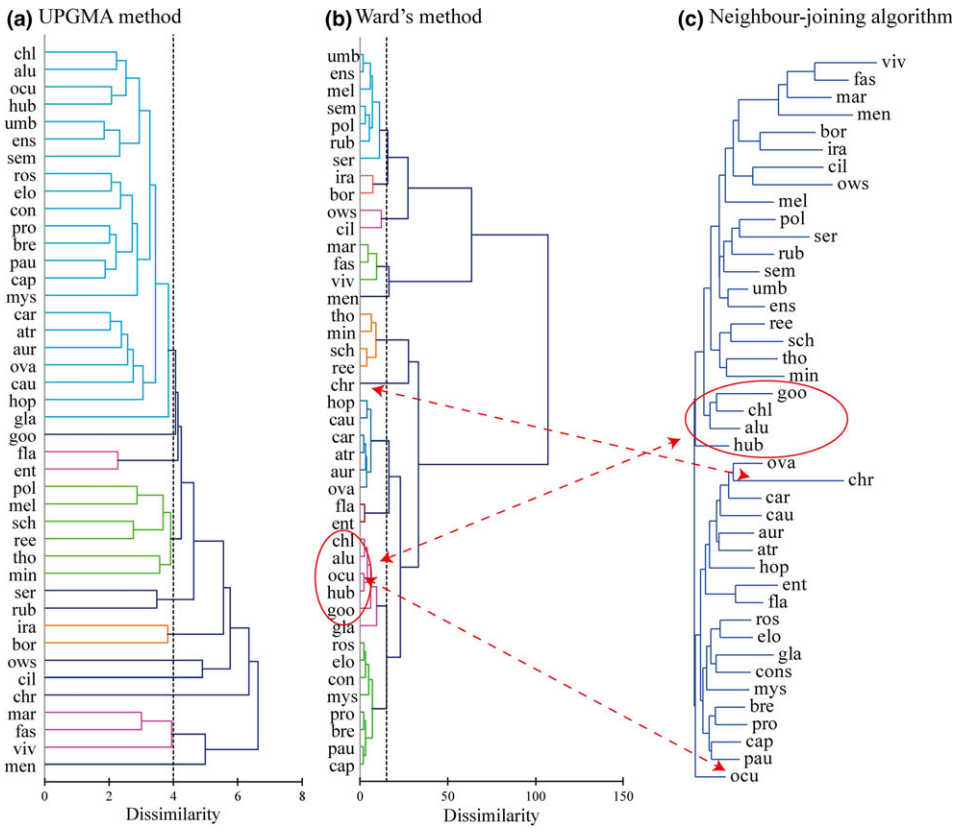

Fig. 3 Clustering otolith shapes from UPGMA (a), Ward (b) and neighbour-joining (c) methods. Circle and arrows indicate the main differences between the Ward and neighbour-joining methods. The species are identified with their acronyms as shown in Table 1 and Fig. 1.

pointed *rostrum*, and short or poorly defined *antirostrum* (*S. rosaceus*, *S. elongatus*, *S. glaucus*, *S. constellatus* and *S. mystinus*); morph IX, fusiform shape with ventral zone more flattened and peaked *rostrum* (*S. brevispinis*, *S. proriger*, *S. capensis* and *S. paucispinis*). The otoliths of *S. hubbsi* and *S. oculatus* appeared in the extreme of the first and second groups; hence, they could be defined as elliptic and fusiform, respectively, with particular characteristics.

Association of phylogeny and otolith shape in *Sebastes*

The Mantel test did not reveal a significant correlation between morphological and phylogenetic distances ($r = 0.013$, $P = 0.702$). Nevertheless, several lineages including *Sebastes* from the north Atlantic (*S. viviparus*, *S. fasciatus*, *S. norvegicus* and *S. mentella*), Clade B (*S. borealis* and *S. iracundus*), *Sebastichthys* (*S. serriceps* and *S. rubrivinctus*), *Zalopyr* (*S. melanostictus* and *S. owstoni*) and *Pteropodus* (*S. chrysomelas*, *S. carnatus*, *S. caurinus*, *S. auriculatus* and *S. atrovirens*) were consistently recovered in the phylogenetic and morphological trees (Figs 1 and 4).

The application of PCoA to the phylogenetic distance matrix indicated high variability in the phylogenetic information. The first three factors only explained 50% of total variation, and up to 20 components were needed to reach up to 96.2% of variation (Table S4). Considering this variability as representative, an RDA between the first 20 morphological and phylogenetic components revealed a weak significant correlation between otolith shape and phylogeny (Pseudo-$F = 1.320$, $P = 0.048$) that explained 56.9% of the variance. The first four axes accounted for 75.1% of the model variability. CVA 1 was significantly correlated with RDA 1 ($r = 0.984$, $P < 0.005$), and to a lower extent, the same occurred between CVA 2 and RDA 2 ($r = 0.741$, $P < 0.005$), CVA 4 and RDA 3 ($r = 0.680$, $P < 0.005$), and between CVA 3 and RDA 4 ($r = 0.542$, $P < 0.01$; Table S5). RDA 1 clearly distinguished the elliptic otolith shape, which was associated with several evolutionary lineages (see above). This axis was associated to the three first values of phylogenetic variables, suggestive of an obvious influence of phylogeny on otolith shape. RDA 2 mainly separated otoliths with small (positive values) and large *rostrum* (negative values), and it was linked to the phylogenetic variables F4, F9 and F10. These associations were

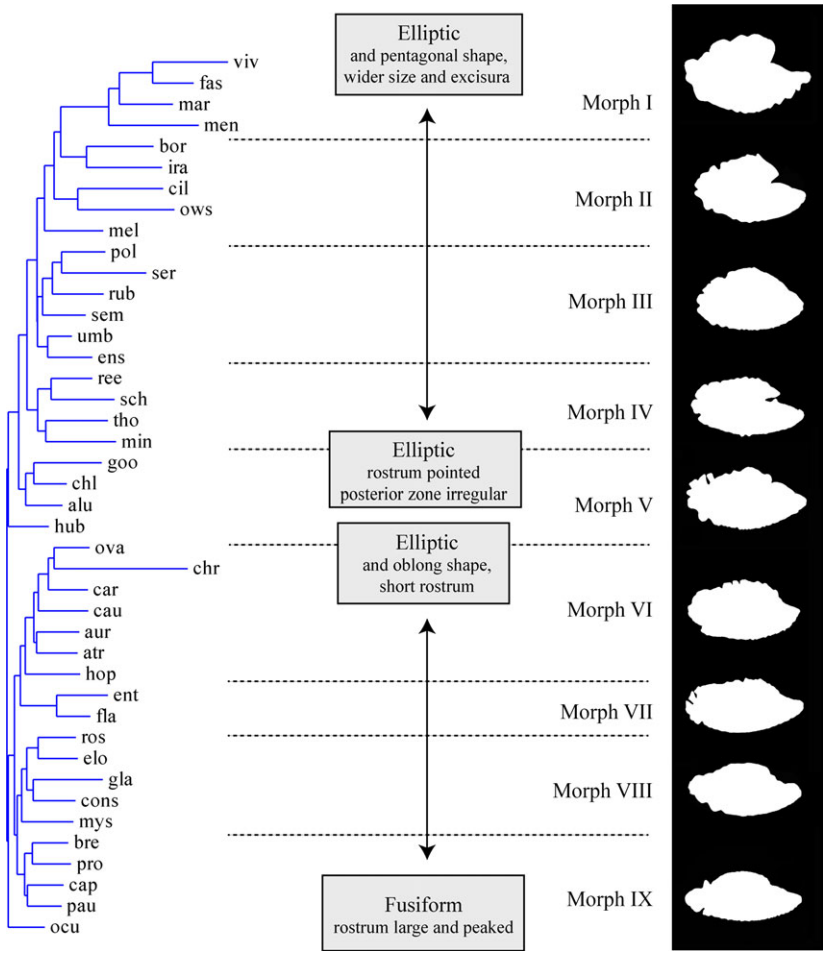

Fig. 4 Otolith morphotypes defined with the neighbour-joining method. The species are identified with their acronyms as shown in Table 1 and Fig. 1.

interpreted as the result of morphological convergence across the diversification of *Sebastes*. In any case, the phylogenetic signal showed a clear relationship with the first four covariates of otolith morphology (Fig. 5, Table S5).

Exogenous and endogenous influences on otolith shape

Independent regression of the ecological characters using the PGLS model with λ fixed to 0 indicated that all factors (age, area, depth and feeding habit) were significantly correlated with the canonical variables (Table 2). CVA 1 presented a higher association with geographical area and depth ($r^2_{adj} = 0.470$, $P < 0.001$; $r^2_{adj} = 0.265$, $P < 0.01$; respectively), whereas CVA 2 was better correlated with feeding habit and age ($r^2_{adj} = 0.216$, $P = 0.017$; $r^2_{adj} = 0.109$, $P = 0.028$; respectively). CVA 4 only showed correlation with feeding habit. The importance of these ecological factors changed when λ was fixed to 1 (Table 2). The geographical area showed a significant association with CVAs 1 and 4 ($P = 0.037$ and $P = 0.011$, respectively), and it was the only variable correlated with the first canonical variable, which represented the highest morphological variability. Depth was the second most important factor, showing a strong significant correlation with CVAs 3 and 4 ($P < 0.001$ in both cases). Finally, feeding habit and age were also correlated with CVAs 3 and 4 ($P = 0.008$ and $P = 0.016$, respectively; Table 2). When the models were built upon the ML estimates of λ, the results indicated that CVA 1 was correlated with area, CVA 2 with depth and age, CVA 3 with depth and CVA 4 with depth and feeding habit. In all cases, there was a strong phylogenetic influence in the estimation of the λ value (Table 2).

Multivariate PGLS analyses of individual CVA axes revealed relationships between ecological traits and specific dimensions of shape variation, which were dissimilar for fixed models (Table 3). When $\lambda = 0$, CVA 1 was correlated to the four ecological traits, CVA 2 was strongly related to the age ($P = 0.007$) and, to lower extents, to the area ($P = 0.01$) and feeding habit

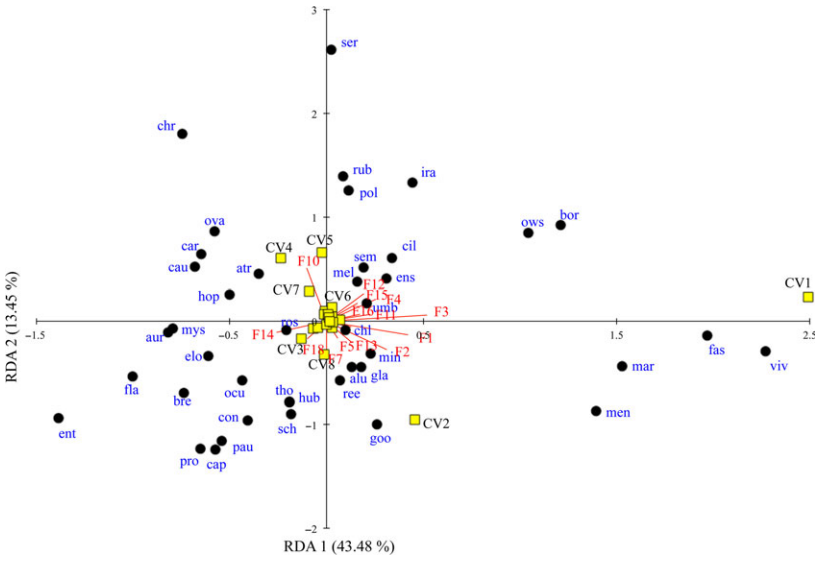

Fig. 5 Redundancy analysis (RDA) between the phylogenetic inertia (red arrows) and canonical variables (yellow squared), and its relationship with the spatial distribution of species (blue points). The species are identified with their acronyms as shown in Table 1 and Fig. 1.

Table 2 Univariate PGLS models for area, depth, feeding habit and age using three null hypotheses: $\lambda = 0$ (no effect of phylogeny), $\lambda = 1$ (assuming Brownian motion) and λ estimated from maximum likelihood method (ML) using the first eight canonical variables.

	$\lambda = 0$		$\lambda = 1$		λ estimated from ML			
Canonical variables	P	r^2_{adj}	P	r^2_{adj}	P	r^2_{adj}	λ	P ($\lambda = 0$)
Area								
CVA 1	**0.000**	0.470	**0.037**	0.233	**0.037**	0.233	1.000	**0.000**
CVA 2	**0.045**	0.219	0.104	0.156	0.230	0.083	0.790	0.119
CVA 3	0.869	−0.129	0.560	−0.030	0.869	−0.129	0.000	0.000
CVA 4	0.108	0.152	**0.011**	0.307	0.196	0.099	0.616	0.055
Depth								
CVA 1	**0.001**	0.265	0.943	−0.026	0.943	−0.026	1.000	**0.000**
CVA 2	**0.038**	0.106	0.882	−0.025	**0.046**	0.075	0.625	**0.004**
CVA 3	0.059	0.088	**0.000**	0.336	**0.000**	0.283	0.837	0.182
CVA 4	0.880	0.001	**0.000**	0.382	**0.000**	0.257	0.939	**0.000**
Feeding habit								
CVA 1	**0.020**	0.209	0.185	0.070	0.185	0.070	1.000	**0.000**
CVA 2	**0.017**	0.216	0.658	−0.045	0.063	0.142	0.421	0.079
CVA 3	0.270	0.041	0.111	0.106	0.270	0.041	0.000	**0.000**
CVA 4	**0.024**	0.198	**0.008**	0.258	**0.032**	0.182	0.752	**0.035**
Age								
CVA 1	0.182	0.024	0.981	−0.029	0.990	−0.029	0.997	**0.000**
CVA 2	**0.028**	0.109	0.706	−0.025	**0.025**	0.115	0.446	**0.039**
CVA 3	0.353	−0.003	**0.016**	0.135	0.066	0.069	0.319	**0.000**
CVA 4	0.148	0.033	0.614	−0.022	0.460	−0.013	0.419	0.073

P: significance; r^2_{adj}: adjusted determination coefficient. For the phylogenetic signal λ, the P-values came from a likelihood ratio test against the null hypothesis of no phylogenetic signal ($\lambda = 0$). Boldface indicates significant relationships ($P < 0.05$).

($P = 0.019$), and CVA 4 was associated with feeding habit ($P = 0.005$) and area ($P = 0.010$; Table 3). No significant correlations involved CVA 3. Nevertheless, CVAs 1 and 4 provided the strongest correlations ($r^2_{adj} = 0.689$ and $r^2_{adj} = 0.507$, respectively). When λ was fixed to 1, CVA 1 was only correlated with feeding habit and area ($P = 0.006$ and $P = 0.007$, respectively), with a high determination coefficient ($r^2_{adj} = 0.535$), whereas CVA 3 was linked to depth ($P < 0.001$) and age ($P = 0.012$), albeit with a low determination coefficient ($r^2_{adj} = 0.261$). Finally, CVA 4 showed a strong ($r^2_{adj} = 0.708$) and significant correlation with area, depth and feeding habit ($P < 0.001$ for all cases; Table 3). When the models were built upon the ML estimates of λ, CVA 1 showed a high phylogenetic signal, with a λ value of 1 and values significantly greater

Table 3 Multivariate PGLS models including age, area, depth and feeding habit using three null hypotheses: $\lambda = 0$ (no effect of phylogeny), $\lambda = 1$ (assuming Brownian motion) and λ estimated from maximum likelihood method (ML) using the first eight canonical variables.

Canonical variables	Age	Area	Depth	Feeding habit	r^2_{adj}	λ	P ($\lambda = 0$)
$\lambda = 0$							
CVA 1	**0.025**	**0.000**	**0.000**	**0.000**	0.689	–	–
CVA 2	**0.007**	**0.010**	0.693	**0.019**	0.468	–	–
CVA 3	0.335	0.419	0.183	0.308	0.085	–	–
CVA 4	0.051	**0.010**	0.784	**0.005**	0.507	–	–
$\lambda = 1$							
CVA 1	0.972	**0.007**	0.902	**0.006**	0.535	–	–
CVA 2	0.658	0.098	0.427	0.252	0.267	–	–
CVA 3	**0.012**	0.189	**0.000**	0.062	0.261	–	–
CVA 4	0.352	**0.000**	**0.000**	**0.000**	0.708	–	–
λ estimated from ML							
CVA 1	0.972	**0.007**	0.902	**0.006**	0.535	1.000	**0.002**
CVA 2	**0.007**	**0.010**	0.693	**0.019**	0.468	0.000	1.000
CVA 3	0.335	0.419	0.183	0.308	0.085	0.000	**0.005**
CVA 4	0.352	**0.000**	**0.000**	**0.000**	0.708	1.000	1.000

r^2_{adj}: adjusted determination coefficient. For the phylogenetic signal λ, the P-value came from a likelihood ratio test against the null hypothesis of no phylogenetic signal ($\lambda = 0$). Boldface indicates significant relationships ($P < 0.05$).

than zero. Feeding habit and area ($P = 0.006$ and $P = 0.007$, respectively) influenced on this canonical variable. CVA 2 showed no phylogenetic signal ($\lambda = 0$), but it was correlated to age, area and feeding habit ($P = 0.007$, $P = 0.010$ and $P = 0.019$, respectively). CVA 4 showed a significant correlation with area, depth and feeding habit ($P < 0.001$ for all variables) for $\lambda = 1$. In all cases, the four ecological variables influenced otolith shape, whereby geographical area and feeding habit were the most relevant factors ($P < 0.01$, for both variables in all models; Table 3).

Discussion

It is widely accepted that the morphological variation in otolith shape is the consequence of a synergy between genetic and environmental factors (Lombarte & Lleonart, 1993; Vignon & Morat, 2010; Vignon, 2015). Similarly, it is well known that these environmental factors also had profound effects on the evolution of rockfishes (Ebeling *et al.*, 1980; Love & York, 2005; Love *et al.*, 2009; Venerus *et al.*, 2013). From these premises, we demonstrate here that both phylogeny and main factors responsible for diversification in rockfishes also have strong effects on the otolith shape. Our findings based on clustering and RDA support the historical hypothesis of an association between phylogenetic divergence and otolith morphology, but we also demonstrate that this alone cannot be used to define phylogenetic relationships (Gaemers, 1984; Nolf, 1985; Schwarzhans, 2014).

Cluster analyses of morphotypes corroborated that the allopatric speciation of some rockfishes favoured the appearance of singular otolith morphs, as it occurred in the case of north Atlantic species (Stransky & MacLellan, 2005). Periods of expansion and contraction of cold water systems, changes in sea level or major alterations of current flow in the Pacific that seemingly contributed to the genetic isolation of some clades (Hyde & Vetter, 2007) were also accompanied by the differentiation in otolith morphs, such as those of the subgenera *Pteropodus* and *Sebastodes*. In fact, PGLS analyses showed an association between otolith morphology, mainly in the first two CVA components, and geographical area, independently of the model used (Brownian or not). The morphospace built from these two components separated the species taking into account otolith width (size and position) and *rostrum* size. These morphological features had already been related to environmental factors and swimming speed (Volpedo & Echeverria, 2003), and apparently they can be reshaped, together with the *antirostrum*, in geographically isolated populations (Reichenbacher *et al.*, 2007; Vignon & Morat, 2010). It is possible that changes in otolith morphology may have happened during the allopatric speciation of the north Atlantic species, which are clearly separated from the Pacific ones (Stransky & MacLellan, 2005; present study). Although *S. mentella* represents a recent divergence (4000–27 000 years ago; Stefánsson *et al.*, 2009), its otolith morphology is markedly specific (80% success of classification).

Numerous studies have demonstrated processes that reshape otoliths depending on foraging strategies (Gagliano *et al.*, 2004; Cardinale & McCormick, 2004). We found that otolith modelling was strongly affected by this factor (PGLS analyses; Tables 2 and 3). Feeding strategies are intrinsically associated with the position of fishes in the water column as manifested by their body shapes. Thus, planktivorous water column dwelling rockfishes have greatly reduced head spines; this is a prominent difference with the benthic-dwelling plesiomorphic representatives of the family, indicating that feeding in the water column is a derived feature (Hyde *et al.*, 2008). Ingram (2011) proposed that a relationship between body shape and habitat exists; however, our findings suggest that morphological convergence of body and otolith shapes are uncoupled. For instance, both morphological and ecological similarities exist between *S. owstoni–ovalis* and *S. hopkinsi* or *S. ciliatus–mystinus* and *S. polyspinis* (Orr & Blackburn, 2004). However, the otolith morphology of *S. owstoni* and *S. ciliatus* are completely different from those of the other two species, which retained higher similarity. The variability of otolith shapes may have an influence on the frequency sensitivities and directional hearing (Gauldie, 1988; Lychakov & Rebane, 2000; Popper

et al., 2005), being advantageous for specific purposes such as locating prey and avoiding predators (Hoin-Radkovsky *et al.*, 1984; Konings, 2001; Ramcharitar *et al.*, 2001). A clear example is given by *S. (Sebastodes) goodei* and *S. (Sebastodes) paucispinis*. Both species are epibenthic and adapted to swimming in the water column, but they have different feeding habits and otolith shapes: *S. goodei* is mainly planktivore and has an otolith with morphotype V, whereas *S. paucispinis* is piscivore and its otolith belongs to morphotype IX. This does not imply that a morphological parallelism between both shapes can occasionally appear, as in *S. alutus* and *S. goodei* (Hyde & Vetter, 2007).

The sensory capability is typical of each species and clearly adapted to endogenous or exogenous factors. Several studies based on otolith morphology have reported the importance of depth in species differentiation (Aguirre & Lombarte, 1999; Tuset *et al.*, 2003; Sadighzadeh *et al.*, 2014), documenting an increase in relative otolith size with depth, up to about 1000 m (Lombarte & Cruz, 2007). The PGLS results (Tables 2 and 3) supported the hypothesis that depth was a key ecological factor for speciation in *Sebastes*, which has been already suggested based on otolith shape (Tuset *et al.*, 2015; Zhuang *et al.*, 2015), body shape (Ingram, 2011) and properties of vision (Sivasundar & Palumbi, 2010). Moreover, increased depth means that fishes spend more time in their specific habitats, have slower metabolism, conserve more energy and therefore live longer (Cailliet *et al.*, 2001). These associations could explain why the age was an essential factor in modelling the contour of otoliths (PGLS analyses; Tables 2 and 3). This is not surprising, because deep-water, long-living species such as *S. viviparus*, *S. fasciatus*, *S. norvegicus* or *S. mentella*, inhabiting the north Atlantic waters, usually have larger, wider and heavier otoliths (Gauldie, 1993; Torres *et al.*, 2000; Lombarte *et al.*, 2003).

Sensory drive is a hypothesis about how communication signals are adapted to work effectively. When visual signalling decreases, differences between signals that affect mating or the detection of predators and prey are increasingly perceived based on sound frequencies, wavelengths of light or olfactory cues (Boughman, 2002). These factors favour qualitatively different traits leading to reproductive isolation among populations and hence to a speciation process. Based on these considerations, we propose that in rockfishes, as in many other deep-sea fish groups, the evolution of communication traits may vary in a bidirectional pattern, governed mainly by depth and feeding habit, demonstrating a sensory trade-off driving the evolutionary process, as limits in the visual field may increase hearing capabilities (Gauldie, 1988; Lombarte & Fortuño, 1992; Popper & Fay, 1993). Cummings (2007) proposed a trade-off model in surfperch on luminance and chromatic detection and predictions about the evolution of colour patterns. In fact, several authors have suggested that sister species and morphotypes of rockfishes undergoing speciation could be distinguished by different colour patterns, which are in turn usually associated with depth distribution (Roques *et al.*, 2001; Hyde *et al.*, 2008; Venerus *et al.*, 2013).

In conclusion, and building from multiple lines of evidence existing for other fish species, first it seems reasonable to assert that otolith shape may be a valuable tool for ecophylogenetic studies where synergistic patterns of ecology, biogeography and macroevolution emerge. Second, the four variables analysed in this study (geographical area, depth distribution, age and feeding habit) contributed to explain the morphological evolution of otoliths in rockfishes, although the geographical area and feeding habit were the most relevant variables in all PGLS models. Third, otolith morphotypes may reflect adaptations to optimize fish survival in the context of different sound environments (Gauldie & Crampton, 2002), which indicate that our results are consistent with the sensory drive hypothesis. Fourth, conversely to other sensory structures, mainly the eyes, the extraction and analyses of otolith contour is a straightforward technique; therefore, sensorial hypotheses may be easily tested in other species to evaluate whether our findings could be generalized.

Acknowledgments

The authors thank many scientists, students and research support personnel who have contributed to the collection and dissection of the otoliths, as well as those who captured and processed the images. Special thanks are reserved to Dmitry Terentiev and Roman Novikov (KamchatNIRO, Petropavlovsk-Kamchatsky, Russia), Ilyas Mukhametov (SakhNIRO, Yuzhno-Sakhalinsk, Russia), Andrei Smirnov (MagadanNIRO, Magadan, Russia), Evgeny Barabanshchikov (TINRO-Center, Vladivostok, Russia), Sergio Martínez, Núria Lombarte, Marina López, Guillermo Aguado and María Cruz Sueiro (CESIMAR, Puerto Madryn, Argentina). We are grateful to Bettina Reichenbacher and David Marjanović for their helpful comments on the manuscript.

References

Aguirre, H. & Lombarte, A. 1999. Ecomorphologic comparisons of sagittae in *Mullus barbatus* and *M. surmuletus*. *J. Fish Biol.* **55**: 105–114.

Anderson, T.J., Syms, C., Roberts, D.A. & Howard, D.F. 2009. Multi-scale fish–habitat associations and the use of habitat surrogates to predict the organisation and abundance of deep-water fish assemblages. *J. Exp. Mar. Biol. Ecol.* **379**: 34–42.

Berkeley, S.A., Chapman, C. & Sogard, S.M. 2004. Maternal age as a determinant of larval growth and survival in a marine fish, *Sebastes melanops*. *Ecology* **85**: 1258–1264.

Boughman, J.W. 2002. How sensory drive can promote speciation. *Trends Ecol. Evol.* **17**: 571–577.

Cailliet, G.M., Andrews, A.H., Burton, E.J., Watters, D.L., Kline, D.E. & Ferry-Graham, L.A. 2001. Age determination and validation studies of marine fishes: do deep-dwellers live longer? *Ex. Gerontol.* **36**: 739–764.

Cardinale, M., Doering-Arjes, P., Kastowsky, M. & Mosegaard, H. 2004. Effects of sex, stock and environment on the shape of known-age Atlantic cod (*Gadus morhua*) otoliths. *Can. J. Fish Aquat. Sci.* **61**: 158–167.

Castonguay, M., Simard, P. & Gagnon, P. 1991. Usefulness of Fourier analysis of otolith shape for Atlantic mackerel (*Scomber scombrus*) stock discrimination. *Can. J. Fish Aquat. Sci.* **48**: 296–302.

Clabaut, C., Bunje, P.M.E., Salzburger, W. & Meyer, A. 2007. Geometric morphometric analyses provide evidence for the adaptive character of the Tanganyikan cichlid fish radiations. *Evolution* **61**: 560–578.

Cummings, M.E. 2007. Sensory trade-offs predict signal divergence in surfperch. *Evolution* **61**: 530–545.

Darriba, D., Taboada, G.L., Doallo, R. & Posada, D. 2012. jModelTest 2: more models, new heuristics and parallel computing. *Nat. Meth.* **9**: 772.

Ebeling, A.W., Larson, R.J., Alevizon, W.S. & Bray, R.N. 1980. Annual variability of reef-fish assemblages in kelp forests off Santa Barbara, California. U.S. *Fish. Bull.* **78**: 361–377.

Endler, J.A. 1992. Signals, signal conditions, and the direction of evolution. *Am. Nat.* **139**: S125–S153.

Endler, J.A. 1993. Some general comments on the evolution and design of animal communication systems. *Philos. Trans. R. Soc. Lond., Ser. B* **340**: 215–225.

Endler, J.A. & Houde, A.E. 1995. Geographic variation in female preferences for male traits in *Poecilia-reticulata*. *Evolution* **49**: 456–468.

Eschmeyer, W.N. & Hureau, J.C. 1971. *Sebastes mouchezi*, a senior synonym of *Helicolenus tristanensis*, with comments on *Sebastes capensis* and zoo-geographical considerations. *Copeia* **1971**: 576–579.

Fay, R.R. & Popper, A.N. 2012. Fish hearing: new perspectives from two "senior" bioacousticians. *Brain Behav. Evol.* **792**: 215–217.

Freckleton, R.P., Harvey, P.H. & Pagel, M. 2002. Phylogenetic analysis and comparative data: a test and review of the evidence. *Am. Nat.* **160**: 712–726.

Froese, R. & Pauly, D. 2015. *FishBase*. World Wide Web electronic publication.

Gaemers, P.A.M. 1984. Taxonomic position of Cichlidae (Pisces, Perciformes) as demonstrated by the morphology of their otoliths. *Neth. J. Zool.* **34**: 566–595.

Gagliano, M. & McCormick, M.I. 2004. Feeding history influences otolith shape in tropical fish. *Mar. Ecol. Progr. Ser.* **278**: 291–296.

Gauldie, R.W. 1988. Function, form and time-keeping properties of fish otoliths. *Comp. Biochem. Physiol. Part A* **91**: 395–402.

Gauldie, R.W. 1993. Continuous and discontinuous growth in the otolith of *Macruronus novaezelandiae* (Merlucciidae: Teleostei). *J. Morph.* **216**: 271–294.

Gauldie, R.W. & Crampton, J.S. 2002. An eco-morphological explanation of individual variability in the shape of the fish otolith: comparison of the otolith of *Hoplostethus atlanticus* with other species by depth. *J. Fish Biol.* **60**: 1204–1221.

Hallacher, L. & Roberts, D. 1985. Differential utilization of space and food by the inshore rockfishes (Scorpaenidae: *Sebastes*) of Carmel Bay, California. *Environ. Biol. Fishes* **12**: 91–110.

Hoin-Radkovsky, I., Bleckmann, H. & Schwartz, E. 1984. Determination of source distance in the surface feeding fish *Pantodon buchholzi* (Pantodontidae). *Ani. Behav.* **32**: 840–851.

Horinouchi, M. & Sano, M. 2000. Food habits of fishes in a *Zostera marina* bed at Aburatsubo, central Japan. *Ichthyol. Res.* **47**: 163–173.

Hyde, J.R. & Vetter, R.D. 2007. The origin, evolution, and diversification of rockfishes of the genus *Sebastes* (Cuvier). *Mol. Phylogenet. Evol.* **44**: 780–811.

Hyde, J.R., Kimbrell, C.A., Budrick, J.E., Lynn, E.A. & Vetter, R.D. 2008. Cryptic speciation in the vermilion rockfish (*Sebastes miniatus*) and the role of bathymetry in the speciation process. *Mol. Ecol.* **17**: 1122–1136.

Ibañez, A.L., Cowx, I.G. & O'Higgins, P. 2007. Geometric morphometric analysis of fish scales for identifying genera, species, and local populations within the Mugilidae. *Can. J. Fish. Aquat. Sci.* **64**: 1091–1100.

Ingram, T. 2011. Speciation along a depth gradient in a marine adaptive radiation. *Proc. R. Soc. Lond. B* **278**: 613–618.

Ingram, T. & Shurin, J.B. 2009. Trait-based assembly and phylogenetic structure in northeast Pacific rockfish assemblages. *Ecology* **90**: 2444–2453.

Jin, X.B. 2006. *Fauna Sinica, Osteichthyes, Scorpaeniformes*. Science Press, Beijing.

Katoh, K., Misawa, K., Kuma, K. & Miyata, T. 2002. MAFFT: a novel method for rapid multiple sequence alignment based on fast Fourier transform. *Nucleic Acids Res.* **30**: 3059–3066.

Kawata, M., Shoji, A., Kawamura, S. & Seehausen, O. 2007. A genetically explicit model of speciation by sensory drive within a continuous population in aquatic environments. *BMC Evol. Biol.* **7**: 99.

Kendall, A.W. Jr. 2000. An historical review of *Sebastes* taxonomy and systematics. *Mar. Fish. Rev.* **62**: 1–23.

Klingenberg, C.P. & Ekau, W. 1996. A combined morphometric and phylogenetic analysis of an ecomorphological trend: pelagization in Antarctic fishes (Perciformes: Nototheniidae). *Biol. J. Linn. Soc.* **59**: 143–177.

Kohavi, R. & Provost, F. 1998. Glossary of terms. *Mach. Learn* **30**: 271–274.

Konings, A. 2001. *Malawi Cichlids in Their Natural Habitat*, 3rd edn. Cichlid Press, El Paso, TX.

Langerhans, R.B. 2010. Predicting evolution with generalized models of divergent selection: a case study with poeciliid fish. *Integr. Comp. Biol.* **50**: 1167–1184.

Legendre, P. & Legendre, L. 1998. *Numerical Ecology*, 2nd English edn. Elsevier Science, Amsterdam.

Linde, M., Palmer, M. & Gómez-Zurita, J. 2004. Differential correlates of diet and phylogeny on the shape of the premaxilla and anterior tooth in sparid fishes (Perciformes: Sparidae). *J. Evol. Biol.* **17**: 941–952.

Lombarte, A. & Castellón, A. 1991. Interspecific and intraspecific otolith variability in the genus *Merluccius* as determined by image analysis. *Can. J. Zool.* **69**: 2442–2449.

Lombarte, A. & Cruz, A. 2007. Otolith size trends in marine fish communities from different depth strata. *J. Fish Biol.* **71**: 53–76.

Lombarte, A. & Fortuño, J.M. 1992. Differences in morphological features of the sacculus of the inner ear of two hakes

(Merluccius capensis and M. paradoxus) inhabits from different depth of sea. *J. Morphol.* **213**: 97–107.

Lombarte, A. & Lleonart, J. 1993. Otolith size changes with body growth, habitat depth and temperature. *Env. Biol. Fish.* **37**: 297–306.

Lombarte, A., Rucabado, J., Matallanas, J. & Lloris, D. 1991. Taxonomía numérica de Nototheniidae en base a la forma de los otolitos. *Sci. Mar.* **55**: 413–418.

Lombarte, A., Torres, G.J. & Morales-Nin, B. 2003. Specific *Merluccius* otolith growth patterns related to phylogenetic and environmental factors. *J. Mar. Biol. Assoc. U.K.* **83**: 277–281.

Lombarte, A., Palmer, M., Matallanas, J., Gómez-Zurita, J. & Morales-Nin, N. 2010. Ecomorphological trends and phylogenetic inertia of otolith sagittae in Nototheniidae. *Environ. Biol. Fishes* **89**: 607–618.

Losos, J.B. 2010. Adaptive radiation, ecological opportunity, and evolutionary determinism. *Am. Nat.* **175**: 623–639.

Love, M.S. & York, A. 2005. A comparison of the fish assemblages associated with an oil/gas pipeline and adjacent seafloor in the Santa Barbara Channel, Southern California Bight. *Bull. Mar. Sci.* **77**: 101–118.

Love, M.S., Morris, P., McCrae, M. & Collins, R. 1990. Life history aspects of 19 rockfish species (Scorpaenidae: *Sebastes*) from the southern California Bight. *NOAA Tech. Rep. NMFS* **87**: 1–38.

Love, M.S., Yoklavich, M. & Thorsteinson, L. 2002. *The Rockfishes of the Northeast Pacific*. University California Press, Los Angeles, CA.

Love, M.S., Yoklavich, M. & Schroeder, D.M. 2009. Demersal fish assemblages in the Southern California Bight based on visual surveys in deep water. *Environ. Biol. Fishes* **84**: 55–68.

Lychakov, D.V. & Rebane, Y.T. 2000. Otolith regularities. *Hear. Res.* **143**: 83–102.

Magnuson-Ford, K., Ingram, T., Redding, D.W. & Mooers, A.Ø. 2009. Rockfish (*Sebastes*) that are evolutionarily isolated are also large, morphologically distinctive and vulnerable to overfishing. *Biol. Conserv.* **142**: 1787–1796.

Mangel, M., Kindsvater, H.K. & Bonsall, M.B. 2007. Evolutionary analysis of life span, competition, and adaptive radiation, motivated by the Pacific rockfishes (*Sebastes*). *Evolution* **61**: 1208–1224.

Mantel, N. 1967. The detection of disease clustering and a generalized regression approach. *Cancer Res.* **27**: 209–220.

Nelson, J.S. 2006. *Fishes of the World*, 4th edn. John Wiley and Sons Inc, Hoboken, NJ.

Nolf, D. 1985. *Otolithi Piscium. Handbook of Paleoichthyology*. Gustav Fischer Verlag, Stuttgart.

Orlov, A.M. & Tokranov, A.M. 2006. Spatial distribution and dynamics of catches of *Sebastes glaucus, S. iracundus* and *S. polyspinis* in Pacific waters off the Kuril Islands and Kamchatka. *J. Ichthyol.* **46**: 625–639.

Orme, D., Freckleton, R., Thomas, G., Petzoldt, T., Fritz, S., Isaac, N. *et al.* 2012. *Caper: Comparative Analyses of Phylogenetics and Evolution in R*. R Package Version 0.5.

Orr, J.W. & Blackburn, J.E. 2004. The dusky rockfishes (Teleostei: Scorpaeniformes) of the North Pacific Ocean: resurrection of Sebastes variabilis (Pallas, 1814) and a redescription of Sebastes ciliatus (Tilesius, 1813). *Fish. Bull.* **102**: 328–348.

Pagel, M. 1999. Inferring the historical patterns of biological evolution. *Nature* **401**: 877–884.

Popper, A.N. & Fay, R.R. 1993. Sound detection and processing by fish: critical review and major research questions. *Brain Behav. Evol.* **41**: 14–38.

Parisi-Baradad, V., Lombarte, A., Garcia-Ladona, E., Cabestany, J., Piera, J. & Chic, Ò. 2005. Otolith shape contour analysis using affine transformation invariant wavelet transforms and curvature scale space representation. *Mar. Freshw. Res.* **56**: 795–804.

Popper, A.N. & Fay, R.R. 1993. Sound detection and processing by fish: critical review and major research questions. *Brain Behav. Evol.* **41**: 14–38.

Popper, A.N. & Fay, R.R. 2011. Rethinking sound detection by fishes. *Hear. Res.* **273**: 25–36.

Popper, A.N., Ramcharitar, J. & Campana, S.E. 2005. Why otoliths? Insights from inner ear physiology and fisheries biology. *Mar. Freshw. Res.* **56**: 497–504.

Price, S.A., Holzman, R., Near, T.J. & Wainwright, P.C. 2011. Coral reefs promote the evolution of morphological diversity and ecological novelty in labrid fishes. *Ecol. Lett.* **14**: 462–469.

Pulcini, D., Costa, C., Aguzzi, J. & Cataudella, S. 2008. Light and shape: a contribution to demonstrate morphological differences in diurnal and nocturnal teleosts. *J. Morph.* **269**: 375–385.

Ramcharitar, J., Higgs, D. & Popper, A.N. 2001. Sciaenid inner ears: a study in diversity. *Brain Behav. Evol.* **58**: 152–162.

Reichenbacher, B., Sienknecht, U., Küchenhoff, H. & Fenske, N. 2007. Combined otolith morphology and morphometry for assessing taxonomy and diversity in fossil and extant killifish (*Aphanius*, †*Prolebias*). *J. Morph.* **268**: 898–915.

Ricklefs, R.E. & Bermingham, E. 2007. Evolutionary radiations of passerine birds in archipelagoes. *Am. Nat.* **169**: 285–297.

Rocha-Olivares, A., Rosenblatt, R.H. & Vetter, R.D. 1999. Molecular evolution, systematics, and zoogeography of the rockfish subgenus *Sebastomus* (*Sebastes*: Scorpaenidae) based on mitochondrial cytochrome *b* and control region sequences. *Mol. Phylogenet. Evol.* **11**: 441–458.

Ronquist, F., Teslenko, M., van der Mark, P., Ayres, D.L., Darling, A., Höhna, S. *et al.* 2012. MrBayes 3.2: efficient Bayesian phylogenetic inference and model choice across a large model space. *Syst. Biol.* **61**: 539–542.

Roques, S., Sevigny, J.M. & Bernatchez, L. 2001. Evidence for broadscale introgressive hybridization between two redfish (genus *Sebastes*) in the North-west Atlantic: a rare marine example. *Mol. Ecol.* **10**: 149–165.

Rüber, L. & Adams, D.C. 2001. Evolutionary convergence of body shape and trophic morphology in cichlids from Lake Tanganyika. *J. Evol. Biol.* **14**: 325–332.

Sadighzadeh, Z., Otero-Ferrer, J.L., Lombarte, A., Fatemi, M.R. & Tuset, V.M. 2014. An approach to unraveling the coexistence of snappers (Lutjanidae) using otolith morphology. *Sci. Mar.* **78**: 353–362.

Schulz-Mirbach, T., Stransky, C., Schilickeisen, J. & Reichenbacher, B. 2008. Differences in otolith morphologies between surface and cave-dwelling populations of *Poecilia mexicana* (Teleostei, Poeciliidae) reflect adaptations to life in an extreme habitat. *Evol. Ecol. Res.* **10**: 537–558.

Schwarzhans, W. 2014. Head and otolith morphology of the genera *Hymenocephalus*, *Hymenogadus* and *Spicomacrurus* (Macrouridae), with the description of three new species. *Zootaxa* **3888**: 1–73.

Seehausen, O., Terai, Y., Magalhaes, I.S., Carleton, K.L., Mrosso, H.D.J., Miyagi, R. *et al.* 2008. Speciation through sensory drive in cichlid fish. *Nature* **455**: 620–626.

Sivasundar, A. & Palumbi, S.R. 2010. Parallel amino acid replacements in the rhodopsins of the rockfishes (*Sebastes* spp.) associated with shifts in habitat depth. *J. Evol. Biol.* **23**: 1159–1169.

Stamatakis, A. 2006. RAxML-VI-HPC: maximum Likelihood-based phylogenetic analyses with thousands of taxa and mixed models. *Bioinformatics* **22**: 2688–2690.

Stefánsson, M.Ö., Sigurdsson, T., Pampoulie, C., Daníelsdóttir, A.K., Thorgilsson, B., Ragnarsdóttir, A. *et al.* 2009. Pleistocene genetic legacy suggests incipient species of *Sebastes mentella* in the Irminger Sea. *Heredity* **102**: 514–524.

Stransky, C. & MacLellan, S.E. 2005. Species separation and zoogeography of redfish and rockfish (genus *Sebastes*) by otolith shape analysis. *Can. J. Fish Aquat. Sci.* **62**: 2265–2276.

Tabatabaei Yazdi, F. & Adriaens, D. 2013. Cranial variation in *Meriones tristrami* (Rodentia: Muridae: Gerbillinae) and its morphological comparison with *Meriones persicus*, *Meriones vinogradovi* and *Meriones libycus*: a geometric morphometric study. *J. Zool. Syst. Evol. Res.* **51**: 239–251.

Torres, G.J., Lombarte, A. & Morales-Nin, B. 2000. Variability of the sulcus acusticus in the sagittal otolith of the genus *Merluccius* (Merlucciidae). *Fish. Res.* **46**: 5–13.

Tuset, V.M., Lombarte, A., González, J.A., Pertusa, J.F. & Lorente, M.J. 2003. Comparative morphology of the sagittae otolith in *Serranus* spp. *J. Fish Biol.* **63**: 1491–1504.

Tuset, V.M., Lombarte, A. & Assis, C.A. 2008. Otolith atlas for the western Mediterranean, north and central Eastern Atlantic. *Sci. Mar.* **72**(S1): 1–198.

Tuset, V.M., Imondi, R., Aguado, G., Otero-Ferrer, J.L., Santschi, L., Lombarte, A. *et al.* 2015. Otolith patterns of rockfishes from the Northeastern Pacific. *J. Morph.* **276**: 458–469.

Venerus, L.A., Ciancio, J.E., Riva-Rossi, C., Gilbert-Horvath, E.A., Gosztonyi, A.E. & Garza, J.C. 2013. Genetic structure and different color morphotypes suggest the occurrence and bathymetric segregation of two incipient species of *Sebastes* off Argentina. *Naturwissenschaften* **100**: 645–658.

Vignon, M. 2015. Disentangling and quantifying sources of otolith shape variation across multiple scales using a new hierarchical partitioning approach. *Mar. Ecol. Progr. Ser.* **534**: 163–177.

Vignon, M. & Morat, F. 2010. Environmental and genetic determinant of otolith shape revealed by a non-indigenous tropical fish. *Mar. Ecol. Progr. Ser.* **411**: 231–241.

Volpedo, A. & Echeverria, D.D. 2003. Ecomorphological patterns of the sagitta in fish on the continental shelf off Argentine. *Fish. Res.* **60**: 551–560.

Winemiller, K.O. 1991. Ecomorphological diversification in lowland fresh-water fish assemblages from five biotic regions. *Ecol. Monogr.* **61**: 343–365.

Zhuang, L., Ye, Z. & Zhang, C. 2015. Application of otolith shape analysis to species separation in *Sebastes* spp. from the Bohai Sea and the Yellow Sea, northwest Pacific. *Environ. Biol. Fish.* **98**: 547–558.

Supporting information

Additional Supporting Information may be found online in the supporting information tab for this article:

Table S1 Sequences of eight loci from Hyde & Vetter (2007) and available in GenBank.

Table S2 Summary of the PCA of the 5th wavelet function in rockfishes.

Table S3 Percentages of classification of rockfishes using leaving-one-out cross-validation in the Canonical Variate Analysis (CVA) on the otolith contour defined by the 5th wavelet.

Table S4 Summary of the PCoA analysis for the phylogenetic signal.

Table S5 Correlation matrix of functions obtained in the Redundancy Analysis (RDA) with canonical variables (CVA 1–20).

Received 17 January 2016; revised 28 May 2016; accepted 27 June 2016